Journal of Applied Fluid Mechanics, Vol. 9, No. 3, pp. 1409-1419, 2016.
Available online at www.jafmonline.net, ISSN 1735-3572, EISSN 1735-3645.
DOI: 10.18869/acadpub.jafm.68.228.24194

Hydromagnetic Mixed Convective Nanofluid Slip Flow past an Inclined Stretching Plate in the Presence of Internal Heat Absorption and Suction

S. P. Anjali Devi and P. Suriyakumar†

Department of Applied Mathematics, Bharathiar University, Coimbatore - 641 046, TamilNadu, India

†*Corresponding Author Email: suriyakumar_08 @yahoo.co.in*

(Received November 8, 2014; accepted August 2, 2015)

ABSTRACT

The steady two-dimensional mixed convective boundary layer flow of nanofluid over an inclined stretching plate with the effects of magnetic field, slip boundary conditions, suction and internal heat absorption have been investigated numerically. Two different types of nanoparticles, namely copper and alumina with water as the base fluid are considered. Similarity transformations are employed to transform the governing nonlinear partial differential equations into coupled non-linear ordinary differential equations. The influence of pertinent parameters such as magnetic interaction parameter, angle of inclination, volume fraction, suction parameter, velocity slip parameter, thermal jump parameter, heat absorption parameter, mixed convection parameter and Prandtl number on the flow and heat transfer characteristics are discussed. A representative set of results are displayed graphically to illustrate the issue of governing parameters on the dimensionless velocity and temperature. Numerical values of skin friction coefficient and the Nusselt number are shown in tabular form. A comparative study between the previously published work and the present results in a limiting sense reveals excellent agreement between them.

Keywords: MHD; Inclined plate; Slip flow; Mixed convection; Suction; Nanofluid.

NOMENCLATURE

a,c	constants
C_f	skin friction coefficient
$(C_p)_f$	specific heat capacity of the base fluid
$(C_p)_s$	specific heat capacity of the nanoparticle
f	dimensionless stream function
g	gravitational acceleration vector
Gr_x	local Grashof number
k_f	thermal conductivity of the base fluid
k_s	thermal conductivity of the nanoparticle
k_{nf}	thermal conductivity of the nanofluid
M^2	magnetic interaction parameter
p	pressure
Pr	Prandtl number
S	suction parameter
b	thermal jump parameter
Hs	heat absorption parameter
T	fluid temperature
$T_w(x)$	surface temperature of the stretching plate
T_∞	ambient temperature
$U_w(x)$	stretching velocity
Re_x	local Reynolds number
(u,v)	velocity components
(x,y)	cartesian coordinates
α	angle of inclination
α_{nf}	thermal diffusivity of the nanofluid
ϕ	volume fraction
β_f	volumetric thermal expansion coefficient of the base fluid.
β_s	volumetric thermal expansion coefficient of the nanoparticle
β_{nf}	volumetric thermal expansion coefficient of the nanofluid
σ	electrical conductivity
ρ_f	density of the base fluid
ρ_s	density of the nanoparticle
ρ_{nf}	density of the nanofluid
γ	velocity slip parameter
μ_f	viscosity of the base fluid
μ_{nf}	viscosity of the nanofluid
ν_f	kinematic viscosity of the base fluid
ν_{nf}	kinematic viscosity of the nanofluid
λ	mixed convection parameter
η	similarity variable
Ψ	stream function
θ	dimensionless temperature

Subscripts

f	fluid
s	nanoparticle
nf	nanofluid

1. INTRODUCTION

In recent era, thermal management of industrial and commercial products has become very much essential and this has attracted the attention of Scientists and engineers. Conventional heat transfer fluids including oil, water and ethylene glycol have low thermal conductivity and thus are inadequate to meet the requirements of today's cooling rate. An innovative technique to improve the thermal conductivities of such fluids is to suspend small solid particles in the base fluids to form slurries. Nanotechnology has been widely used since the material with size of nanometres possesses unique physical and chemical properties.

The term nanofluid was first coined by Choi (1995) where he described the future and hope of this cation of nanotechnology. Nanofluids are a novel class of nanotechnology-based heat transfer fluids engineered by dispersing nanometre-scale solid particles with typical length scales on the order of 1-100nm in traditional heat transfer fluids. The main characteristics of the nanofluids have better thermo physical properties such as high thermal conductivity, minimal clogging in flow passage, long term stability and homogeneity. The study of nanofluids has several industrial and engineering applications such as chemical production, solar and power plant cooling, cooling of transformer oil, production of microelectronics, automotive and air conditioning cooling, advanced nuclear systems, nano-drug delivery, micro fluidics, transportation, biomedicine, solid-state lighting and manufacturing.

Further, the mixed convective heat transfer has been deriving considerable attention due to its essential role in various applications such as electronic devices, heat exchangers, nuclear reactors, food processing and solar collectors. However, Convection along inclined surfaces, bluff bodies has been receiving attention because of many industrial applications in fields such as electroplating, chemical processing of heavy metals, ash or scrubber waste treatment etc.

Many recent studies have been focused on the problem of magnetic effect on laminar mixed convection boundary layer flow over a stretching surface which has attracted considerable attention during the last few decades. Some of the industrial examples of the problem are extrusion processes, cooling of nuclear reactors, glass fibre production, hot rolling, wire drawing and crystal growing. Moreover, the fluids exhibiting boundary slip find applications in technological applications such as in the polishing of the artificial heart valves and internal cavities. Motivated by all these applications, the present work is dealt with a study concerned with these.

Mucoglu and Chen (1979) analyzed the mixed convection along an inclined flat plate when the plate is subjected to a uniform heat flux. The fluid stream and heat transport due to a stretching boundary is important in the extrusion process. Numerous researchers have analyzed the hydromagnetic flow over inclined stretching plate considering various physical situations and few of them are Chamkha and Rahim (2001), Ramadan and Chamkha (2003), Alam *et al*. (2006), Aydin and Kaya (2009) and Noor *et al*. (2012). Ishak *et al*. (2008) studied the steady two dimensional magnetohydrodynamic flow of an incompressible viscous and electrically conducting fluid over a stretching vertical sheet with the variable temperature. The comprehensive survey that took into account of the slip boundary conditions over a stretching surface were investigated by Andersson (2002), Wang (2002), Martin and Boyd (2006), Cao and Baker (2009), Fang *et al*. (2009), Wang (2009), Aziz (2010) and Hayat *et al*. (2011).

Recently, many articles concerning the study of two dimensional convective heat transfer of nanofluids have been published. The recent book by Das *et al*.(2007) and more recent review paper by Kakac and Pramuanjaroenkij (2009) examined an excellent aggregation of the study done on nanofluids. Oztop and Abu-Nada (2008) and Abu Nada and Oztop (2009) numerically analyzed the effects of inclination angle on natural convection heat transfer and fluid flow in a two dimensional enclosure filled with copper-water nanofluid. The two dimensional, steady boundary layer flow of a nanofluid past a moving flat plate in a uniform free stream was solved numerically using a Keller box method by Bachock *et al*. (2010). Khan and Pop (2010) proposed the laminar fluid flow, which results from the stretching of a plane surface in a nanofluid. The model used for the nanofluid incorporates the effects of Brownian motion and thermophoresis. The two dimensional convective laminar boundary layer flow of nanofluid over a flat plate was analyzed by Anjali Devi and Julie Andrews (2011) and it was found out that suspended nanoparticles enhance the heat transfer capacity of the fluids. Hassani *et al*. (2011) solved analytically the development of the steady boundary layer flow of a nanofluid past a stretching sheet using the Homotopy analysis method. The convective flow and heat transfer of an incompressible viscous nanofluid past a semi-infinite vertical stretching sheet in the presence of a magnetic field was examined by Hamad (2011). He found that the heat transfer rates decrease as the nanoparticle volume fraction increases.

The heat transfer characteristics of steady two-dimensional boundary layer flow over a moving surface in a nanofluid with suction or injection are numerically analyzed by Bachok *et al*. (2012) applying an implicit finite difference method. The outcomes suggest that the suction delays the boundary layer separation, while the injection accelerates it. Das (2012) demonstrated the convective heat transfer performance of nanofluids over a permeable stretching surface in the presence of partial slip, thermal buoyancy and temperature dependent internal heat generation or absorption.

Turkyilmazoglu (2012) studied analytically the MHD flow and thermal transport characteristics of nanofluid flow past a continuously stretching or

shrinking permeable sheet in the presence of velocity slip and temperature jump. A two dimensional steady hydromagnetic slip flow of water based nanofluids over a wedge with convective surface, taking into account the effects of heat generation (or absorption) was executed by Rahman *et al*. (2012). Noghrehabadi *et al*. (2012) investigated the heat transfer of magnetohydrodynamic viscous nanofluids in the presence of Brownian motion and thermophoresis over an isothermal stretching sheet.

Recently, Sharma *et al*. (2013) examined the partial slip flow and heat transfer of a nanofluid over a stretching sheet using finite element method. Flow and heat transfer of nanofluid over a permeable MHD stretching surface was presented by Keshtkar and Amiri (2013). They observed that, the Nusselt number and heat transfer increase due to nanoparticles in the base fluid. Srikanth *et al*. (2013) investigated theoretically the MHD flow of a nanofluid past an inclined permeable plate with constant heat source and thermal radiation. The steady, mixed convective, two-dimensional laminar hydromagnetic boundary layer flow of copper-water and alumina-water nanofluids over an inclined flat plate with an angle of inclination in the presence of uniform transverse magnetic field was analyzed by Anjali Devi and Suriyakumar (2013). The effects of internal heat generation or absorption on free convection flow of a nanofluid past an isothermal inclined plate have been investigated by Akilu and Narahari (2014). Haile and Shankar (2015) studied the hydromagnetic boundary layer flow of water based nanofluids over a moving permeable flat plate.

As per author's knowledge since no investigations have been made so far on the effects of slip and sink over the mixed convective MHD flow over an inclined porous surface, the numerical investigation on hydromagnetic mixed convective nonlinear nanofluid slip flow past an inclined permeable stretching plate in the presence of heat absorption has been made in this work. By using suitable similarity variables, the governing partial differential equations of the problem are converted into coupled ordinary differential equations and are solved numerically using MATLAB R2012b. The effects of the various non-dimensional parameters namely angle of inclination, magnetic interaction parameter, volume fraction, suction parameter, velocity slip parameter, thermal jump parameter, heat absorption parameter, mixed convection parameter and Prandtl number over the flow field and temperature distribution are discussed with the aid of graphs. The numerical values of skin friction coefficient and reduced Nusselt number are also analyzed with the help of tables.

2. FORMULATION OF THE PROBLEM

The steady, two-dimensional, incompressible, laminar, hydromagnetic mixed convective nanofluid slip flow past an inclined stretching plate in the presence of heat absorption and suction is considered. The plate is inclined at an angle of inclination α with the horizontal and is of infinite length. The stretching velocity of the plate is linear, which is taken as $u = U_w(x) = ax$, where a is a constant. The Cartesian coordinates (x, y) are chosen such that x -axis is chosen along the plate and the y-axis is chosen perpendicular to the plate which is shown in Fig.1. The gravitational acceleration g is acting downward. There is a constant suction velocity v_w normal to the stretching plate. The fluid is water-based nanofluid containing different types of nanosolid particles, say copper (Cu) and Alumina (Al_2O_3). The stretching surface of the temperature is $T_w(x) = T_\infty + cx$ and the ambient temperature is T_∞. A uniform magnetic field of strength $\overrightarrow{B_0}$ is applied normal to the plate. The induced magnetic field is assumed to be small compared to the applied magnetic field; so that it can be neglected. It is further assumed that the base fluid and the suspended nanoparticles are in thermal equilibrium. Since the flow is steady, $\nabla X\vec{E} = 0$ and in the absence of surface charge density $\nabla.\vec{E} = 0$ which leads to the fact that $\vec{E} = 0$. The thermophysical properties of the nanofluids are given in Table 1. Further, the viscous and Joule's effects are neglected in the energy equation. Following the lines of Mucoglu and Chen (1979)[vide Gebhart *et al*.(1988)] the boundary layer equations reduce to

$$\frac{\partial u}{\partial x} + \frac{\partial v}{\partial y} = 0 \tag{1}$$

$$u\frac{\partial u}{\partial x} + v\frac{\partial u}{\partial y} = \nu_{nf}\frac{\partial^2 u}{\partial y^2} + \frac{g(\rho\beta)_{nf}(T-T_\infty)sin\alpha}{\rho_{nf}} - \frac{\sigma B_0^2 u}{\rho_{nf}} \tag{2}$$

$$u\frac{\partial T}{\partial x} + v\frac{\partial T}{\partial y} = \alpha_{nf}\frac{\partial^2 T}{\partial y^2} + \frac{Q_0(T-T_\infty)}{(\rho C_p)_{nf}} \tag{3}$$

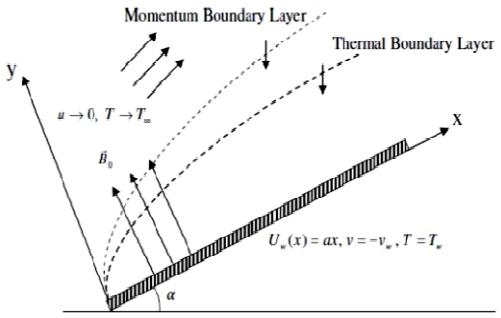

Fig. 1. **Schematic diagram of the problem**.

The boundary conditions for the velocity and temperature of this problem are given by:

$$At\ y = 0, u = U_w(x) + h_1\frac{\partial u}{\partial y}, v = -v_w,$$

$$T = T_w(x) + h_2\frac{\partial T}{\partial y}$$

$$As\ y \to \infty,\ u \to 0,\ T \to T_\infty \tag{4}$$

Here u and v are velocity components in x and y directions respectively, $U_w(x) = ax$ is the

stretching velocity, h_1 is the velocity slip factor, h_2 is the thermal jump factor, v_w is the suction, B_0 is the strength of the magnetic field and Q_0 is the heat absorption coefficient ($Q_0 < 0$).

For the present study, water has been considered as the base fluid with Pr = 6.2 at 25° C. The nanofluid considered is water mixed with solid spherical copper and aluminium nanoparticles. The effective density, heat capacity, dynamic viscosity, thermal expansion coefficient, thermal diffusivity and the thermal conductivity of the nanofluids are given by

$$\rho_{nf} = (1-\phi)\rho_f + \phi\rho_s ,$$

$$\left(\rho C_p\right)_{nf} = (1-\phi)\left(\rho C_p\right)_f + \phi\left(\rho C_p\right)_s ,$$

$$\mu_{nf} = \frac{\mu_f}{(1-\phi)^{2.5}}$$

$$(\rho\beta)_{nf} = (1-\phi)(\rho\beta)_f + \phi(\rho\beta)_s ,$$

$$\alpha_{nf} = \frac{k_{nf}}{\left(\rho C_p\right)_{nf}},$$

$$\frac{k_{nf}}{k_f} = \frac{k_s + 2k_f - 2\phi\left(k_f - k_s\right)}{k_s + 2k_f + \phi\left(k_f - k_s\right)}$$

Table 1 Thermo Physical properties of base fluid water, copper and alumina nanoparticles at 25°C (Oztop and Abu Nada (2008))

	ρ (Kg/m^3)	C_p (J/Kg.K)	K (W/m.K)	β x10^5 k^{-1}
Water	997.1	4179	0.613	21
Copper	8933	385	400	1.67
Alumina	3970	765	40	0.85

In order to seek the solution of the problem, the following dimensionless variables are introduced:

$$\psi(x,y) = x\sqrt{av_f}\,F(\eta), \quad \eta = y\sqrt{\frac{a}{v_f}} ,$$

$$\theta(\eta) = \frac{T-T_\infty}{T_w-T_\infty} \tag{5}$$

where $\psi(x,y)$ is the stream function such that it satisfies Eq.(1) with $u = \frac{\partial\psi}{\partial y}$, $v = -\frac{\partial\psi}{\partial x}$ and θ is the dimensionless temperature. It is obtained that

$$u = U_w(x)F'(\eta) , \qquad v = -\sqrt{av_f}\,F(\eta) \tag{6}$$

The momentum and energy equations together with the boundary conditions can be written as

$$F''' + (1-\phi)^{2.5}\left\{(FF'' - F'^2)\left[(1-\phi) + \phi\left(\frac{\rho_s}{\rho_f}\right)\right] - M^2F' + \lambda\left[(1-\phi) + \phi\frac{(\rho\beta)_s}{(\rho\beta)_f}\right]\theta\sin\alpha\right\} = 0 \tag{7}$$

$$\frac{1}{Pr}\frac{k_{nf}}{k_f}\theta'' + \left[(1-\phi) + \phi\frac{\left(\rho C_p\right)_s}{\left(\rho C_p\right)_f}\right](F\theta' - F'\theta) + H_s\theta = 0 \tag{8}$$

with boundary conditions as follows :

$$At\ \eta = 0, \quad F(\eta) = S, F'(\eta) = 1 + \gamma F''(0) ,$$

$$\theta(\eta) = 1 + b\theta'(0)$$

$$As \quad \eta \to \infty,\ F'(\eta) = 0,\ \theta(\eta) = 0 \tag{9}$$

Here the primes denote differentiations with respect to η. The corresponding dimensionless group that appears in the governing equations are defined by

$$Pr = \frac{v_f}{\alpha_f} , \quad (Re_x)_f = \frac{U_w(x)x}{v_f} , \qquad M^2 = \frac{\sigma B_0^2}{a\rho_f}$$

$$(Gr_x)_f = \frac{g\beta(T_w - T_\infty)x^3}{v_f^2} , S = \frac{v_w}{\sqrt{av_f}} , \ \gamma = h_1\sqrt{\frac{a}{v_f}} ,$$

$$\lambda = \frac{(Gr_x)_f}{Re_x^2} = \frac{g\beta_f c}{a} = const., \ b = h_2\sqrt{\frac{a}{v_f}}$$

$$H_s = \frac{Q_0}{a\left(\rho C_p\right)_f}$$

3. NUMERICAL SOLUTION

Equations (7) and (8) with boundary conditions (9) constitute a non-linear boundary value problem and cannot be solved analytically. So numerical solution of the non-linear problem is sought. The system of coupled non-linear differential equations with the boundary conditions are solved numerically in the symbolic computation software MATLAB R2012b (bvp4c) for several values of the physical parameters such as magnetic interaction parameter, angle of inclination, volume fraction, suction parameter, heat absorption parameter, velocity slip parameter and thermal jump parameter with fixed values of Prandtl number and mixed convection parameter.

The coupled non-linear boundary value problem of third order in F and second order in θ has been reduced to a system of simultaneous equations of first order for five unknowns. Thus, we set y_1= F, y_2= F', y_3= F'', y_4= θ , y_5 = θ'. The reduced systems of equations are as follows:

$$y_1' = y_2$$

$$y_2' = y_3$$

$$y_3' = -(1-\phi)^{2.5}\{(y_1y_3 - y_2^2)\left[\left((1-\phi) + \phi\frac{\rho_s}{\rho_f}\right)\right] - M^2y_2 + \lambda\left[(1-\phi) + \phi\frac{(\rho\beta)_s}{(\rho\beta)_f}\right]y_4 sin\alpha\}$$

$$y_4' = y_5$$

$$y_5' = -Pr\frac{k_f}{k_{nf}}\{(y_1y_5 - y_2y_4)\left[(1-\phi) + \phi\frac{\left(\rho C_p\right)_s}{\left(\rho C_p\right)_f}\right] + H_sy_4\}$$

and the corresponding initial conditions are

$$y_1(0) = S, \ y_2(0) = 1 + h_1g_1, \qquad y_3(0) = g_1,$$

$$y_4(0) = 1 + h_2g_2, \ y_5(0) = g_2$$

where g_1 and g_2 are unknown which are to be obtained. Note that bvp4c uses a collocation method and requires an initial guess for the desired solution for the ordinary differential equations (7) and (8). In

order to make an appropriate guess we start with a set of parameter values for which solution was known and progress until we obtain the solution of our problem. The above procedure is repeated until we get the results up to the desired degree of accuracy is 10^{-6}.

The asymptotic boundary conditions given by Eq.(9) were replaced by using a value of 15 for the similarity variable η_{max} as follows.

$$\eta_{max} = 15, \qquad F'(15) = 0, \qquad \theta(15) = 0$$

The choice of $\eta_{max} = 15$ ensured that all numerical solutions approached the asymptotic values correctly. The numerical values for skin friction coefficient and the reduced Nusselt number are also obtained and are tabulated for different values of M^2, ϕ, α, γ, S, b and Hs.

Concerning this study, the physical quantities of practical interest are the skin friction coefficient C_f and the local Nusselt number Nu_x and are defined as

$$C_f = \frac{\tau_w}{\rho_f (U_w(x))^2} \text{ and } Nu_x = \frac{x q_w}{k_f (T_w - T_\infty)} \qquad (10)$$

where the wall shear stress τ_w and the surface heat flux q_w are given by

$$\tau_w = \mu_{nf} \left(\frac{\partial u}{\partial y}\right)_{y=0} \text{ and } q_w = -k_{nf} \left(\frac{\partial T}{\partial y}\right)_{y=0} \qquad (11)$$

Substituting Eq.(11) in Eq.(10), the skin friction coefficient and reduced Nusselt number are obtained as

$$C_f (Re_x)_f^{1/2} = \frac{1}{(1-\phi)^{2.5}} F''(0) \qquad (12)$$

$$Nu_x (Re_x)_f^{-1/2} = -\frac{k_{nf}}{k_f} \theta'(0) \qquad (13)$$

Table 2 Comparison of $F''(0)$ and $-\theta'(0)$ for various values of M^2 when $\gamma = 0$, $S = 0, \phi = 0$, $Hs = 0, b = 0, \alpha = 90^0$, $Pr = 1$ and $\lambda = 1$.

M^2	Ishak *et al*.(2008) (when m =1 and n =1)		Present Results	
	$F''(0)$	$-\theta'(0)$	$F''(0)$	$-\theta'(0)$
0.0	-0.5607	1.0873	-0.5608	1.0873
0.1	-0.5658	1.0863	-0.5659	1.0863
0.2	-0.5810	1.0833	-0.5810	1.0833
0.5	-0.6830	1.0630	-0.6830	1.0630
1.0	-1.0000	1.0000	-1.0000	1.0000
2.0	-1.8968	0.8311	-1.8968	0.8311
5.0	-4.9155	0.4702	-4.9155	0.4703

4. RESULTS AND DISCUSSION

Physically realistic numerical values were assigned to the pertinent parameters in the system in order to gain an insight into the flow structure with respect to velocity, temperature, skin friction coefficient and the reduced Nusselt number. Two different types of nanoparticles namely copper and alumina with water as the base fluid are considered. The Prandtl number is kept constant at Pr= 6.2 and the mixed convection parameter is fixed at $\lambda = 1.5$ for different values of physical parameters such as M^2 = 0,1,2,4, $\alpha = 0^0, 30^0, 45^0, 60^0$, ϕ = 0.0,0.01, 0.05,0.1, γ =0.0,0.1,0.2,0.3, b = 0.0,0.1,0.2,0.3, S = 0.1,0.3,0.5,0.7 and Hs = 0,-1,-3,-5. The numerical solutions are illustrated by means of graphs and tables.

The accuracy of the numerical method was validated by direct comparisons with the numerical results reported earlier by Ishak *et al*. (2008) for a regular fluid and in the absence of volume fraction, suction parameter, slip parameters and heat absorption, the numerical results are presented in Table 2. It is seen from this table that excellent agreement between the results exists which justifies our numerical scheme in the case of m=1 and n=1 to that of Ishak *et al*. (2008).

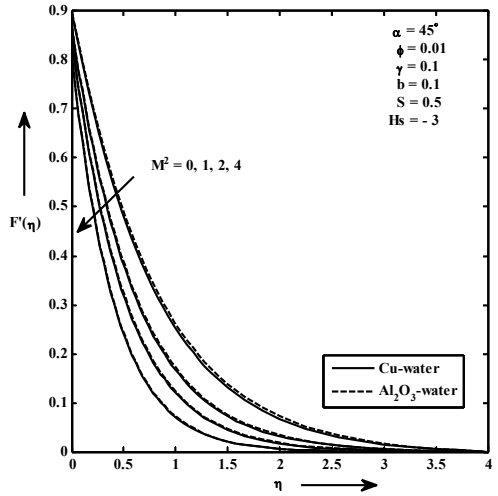

Fig. 2. Dimensionless Velocity profiles for different M^2.

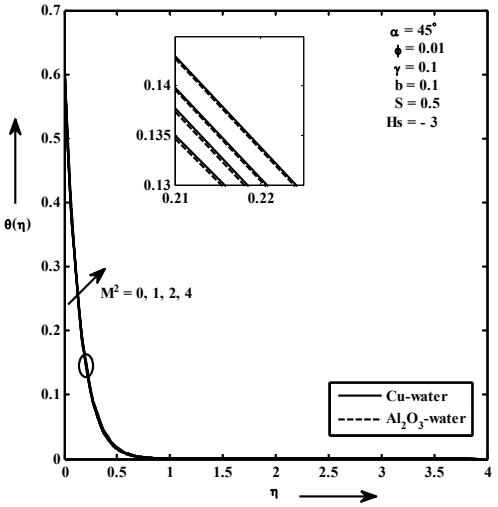

Fig. 3. Temperature distribution for different M^2.

Figs.(2)-(13) represent typical numerical results based on the numerical solution of Eqs. (7) - (9).

These results were held to illustrate the influence of the magnetic interaction parameter, angle of inclination, volume fraction, velocity slip parameter, thermal jump parameter, suction parameter and heat absorption parameter over the velocity and temperature in both the cases of copper-water and alumina-water nanofluids.

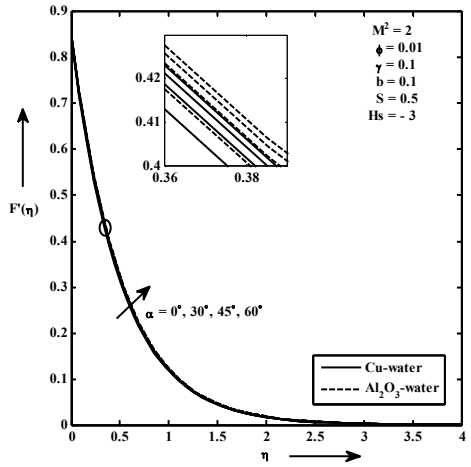

Fig. 4. Dimensionless velocity profiles for different α

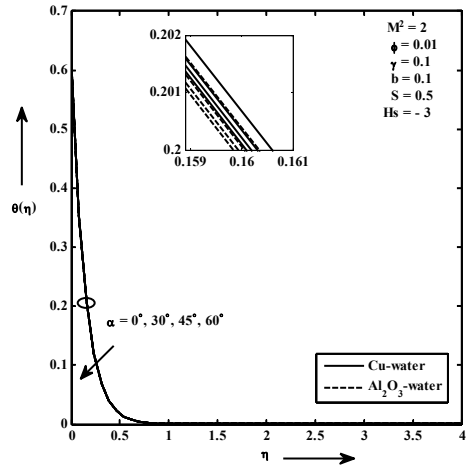

Fig. 5. Temperature distribution for different α.

Figs. 2 and 3 depict the dimensionless velocity and temperature distribution for various values of the magnetic interaction parameter for both copper-water and alumina-water nanofluids when $\phi = 0.01$. In general, velocity and temperature profiles tend to zero asymptotically in the direction of the stretching plate. The presence of transverse magnetic field sets in Lorentz force effect, which results in the retarding effect on the velocity field. As the values of magnetic interaction parameter M^2 increase, the retarding force increases and consequently the velocity gets decelerated. The Lorentz force increases the nanofluid resistance which causes an increase in the temperature when M^2 increases. Thus the presence of the magnetic field reduces the momentum boundary layer thickness while it enhances the thermal boundary layer thickness for both types of nanofluids. However, an increment in thermal boundary layer is not significant amount for both copper-water and alumina-water nanofluids.

The influence of inclination angle on dimensionless velocity and temperature distribution for specific parameters for both copper-water and alumina-water nanofluids are portrayed through Figs.4 and 5. It is observed from Fig.4 that for increasing angle of inclination, the velocity gets accelerated. This is because the angle of inclination increases the effect of buoyancy force due to the thermal diffusion by a factor of $sin\alpha$. Consequently, the driving force to the fluid increases as a result, velocity of the nanofluid increases. It is also elucidated that its effect enhances the momentum boundary layer thickness with increasing values of α. When α increases, the temperature and the thermal boundary layer thickness reduce for both copper-water and alumina-water nanofluids as shown in Fig.5. However, the change is not significant.

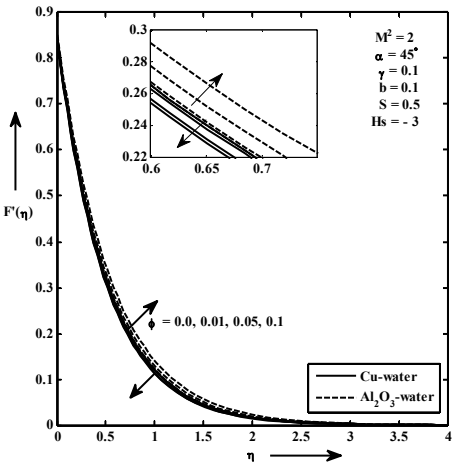

Fig. 6. Dimensionless velocity profiles for different ϕ.

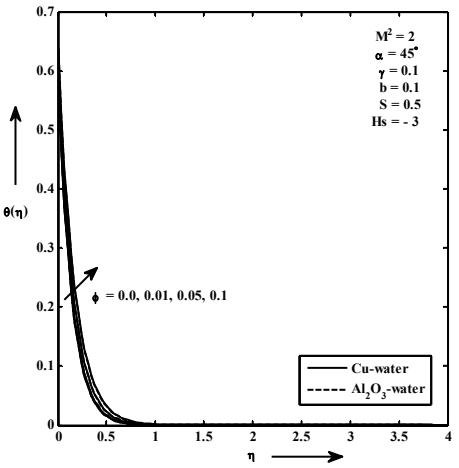

Fig. 7. Temperature distribution for different ϕ.

Fig.6 shows the graphical representation of the velocity for various values of the volume fraction of copper and aluminium nanoparticles. When the volume fraction of copper nanoparticles increases, the velocity in the boundary layer decreases and this

is because of the more collisions between solid particles and consequently lead to the reduction of nanofluid effective velocity.

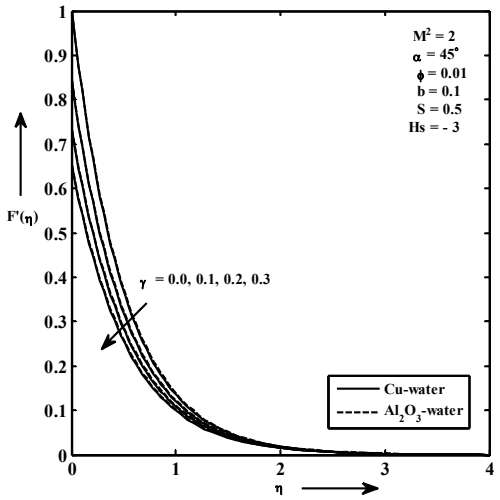

Fig. 8. Dimensionless velocity profiles for different γ.

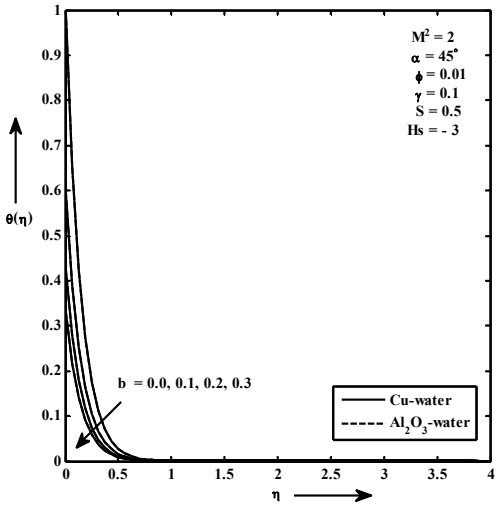

Fig. 9. Temperature distribution for different b.

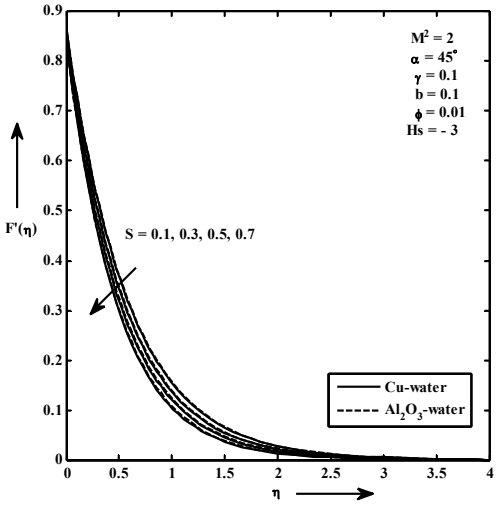

Fig. 10. Dimensionless velocity profiles for different S.

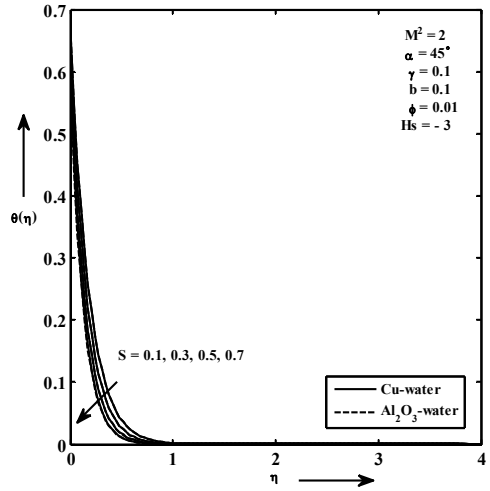

Fig. 11. Temperature distribution for different S.

In contrary, the nanofluid velocity gets accelerated by increasing the volume fraction of aluminium nanoparticles. This is because the density of alumina is less compared to copper, so that it accelerates the velocity due to increasing aluminium nanoparticles. It is interesting to note that the nanofluid momentum boundary layer thickness decreases slightly by adding the number of copper nanoparticles while the reverse is true for the momentum boundary layer in the case of aluminium nanoparticles. The consequence of the solid volume fraction ϕ for copper-water and alumina-water nanofluids over the temperature distribution is indicated in Fig.7. Increasing values of the solid volume fraction lead to both the enhancement in the temperature and as well as in the thermal boundary layer thickness for both types of nanofluids and temperature distribution tends asymptotically to zero as the distance increases from the boundary. This agrees with the physical behavior that when the volume fraction of copper and alumina increases, the thermal conductivity increases and hence the thickness of the thermal boundary layer also increases.

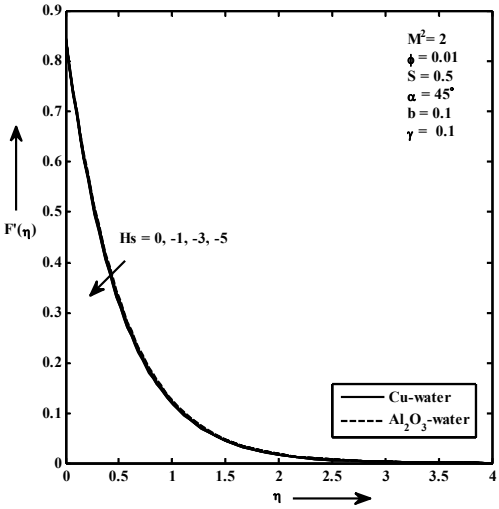

Fig. 12. Dimensionless velocity profiles for different Hs.

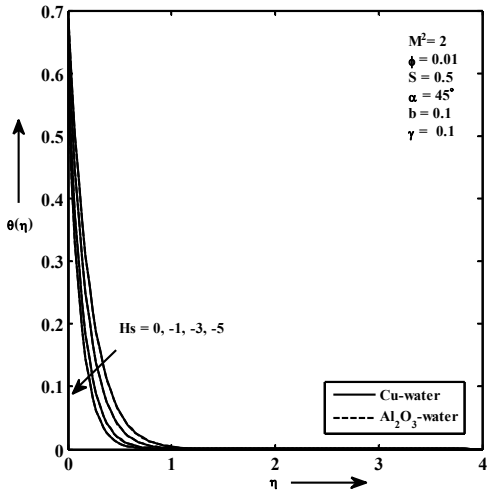

Fig. 13. Temperature distribution for different Hs.

In Fig. 8, the dimensionless velocity for various values of velocity slip parameter for both copper-water and alumina-water nanofluids are represented. It is clear from the figure that the velocity component in the direction of wall is reduced with an increase in the velocity slip parameter for both the nanofluids and decreases asymptotically to zero at the edge of the momentum boundary layer. This yields a decrease in the boundary layer thickness. Thus, the momentum boundary layer thickness is reduced as the velocity slip parameter increases for both types of nanofluids and as a result, the velocity gets decelerated. Fig.9 reveals the influence of thermal jump parameter on temperature distribution for both copper-water and alumina-water nanofluids. As the thermal jump parameter increases, less heat is transferred from the plate to the fluid and hence the temperature reduces for both types of nanofluids whereas change in the velocity of the fluid is not substantial with the increase of the effectiveness of the thermal jump boundary condition.

Figs.10 and 11 demonstrate the effect of the variation of suction parameter on the velocity and temperature distribution in both copper-water and alumina-water nanofluids. In the case of suction the heated fluid is pushed towards the plate where the buoyancy forces can act to retard the fluid. This effect acts to decelerate the velocity. It is recognized that the effect of suction is to bring the fluid closer to the surface and hence to reduce both the momentum and the thermal boundary layer thickness for both types of nanofluids. The effect of the heat absorption parameter on the velocity for both copper-water and alumina-water nanofluids is presented in Fig.12. When the heat absorption intensifies, the velocity is found to suppress due to the reduction in the buoyancy force. Thus, the momentum boundary layer thickness of the nanofluid decreases. Fig.13 predicts the effect of heat absorption parameter on the temperature distribution for both types of nanofluids within the boundary layer. Owing to the presence of heat absorption (Hs < 0), it is apparent that there is a decrease in the thermal state of the fluid. As expected, heat absorption provides a decrease in the temperature of the fluid. Therefore, the thermal boundary layer thickness also reduces due to the increase in the heat absorption parameter.

Table 3 Variation in $\frac{1}{(1-\phi)^{2.5}}F''(0)$ for Copper-water and alumina-water nanofluids for different values of $M^2, \alpha, \phi, \gamma, b, S$ and H_s when $\lambda = 1.5$ and Pr = 6.2

M^2	$\frac{1}{(1-\phi)^{2.5}}F''(0)$	
	Cu- water nanofluid	Al_2O_3- water nanofluid
	$\alpha = 45^0$, ϕ = 0.01, γ = 0.1, b = 0.1, S = 0.5, Hs = -3	
0	-1.086133	-1.057378
1	-1.395815	-1.374332
2	-1.624076	-1.606043
4	-1.966317	-1.951901
α	M^2 = 2, ϕ = 0.01, γ = 0.1, b = 0.1, S = 0.5, Hs = -3	
0^0	-1.684783	-1.666549
30^0	-1.641822	-1.623731
45^0	-1.624076	-1.606043
60^0	-1.610477	-1.592489
ϕ	M^2 = 2, $\alpha = 45^0$, γ = 0.1, b = 0.1, S = 0.5, Hs = -3	
0.00	-1.574249	-1.574249
0.01	-1.624076	-1.606043
0.05	-1.831870	-1.740495
0.10	-2.113713	-1.926910
γ	M^2 =2, $\alpha = 45^0$, ϕ = 0.01, b = 0.1, S = 0.5, Hs = -3	
0.0	-1.995563	-1.967426
0.1	-1.624076	-1.606043
0.2	-1.374991	-1.362349
0.3	-1.194914	-1.185518
b	M^2 = 2, $\alpha = 45^0$, ϕ = 0.01, γ = 0.1, S = 0.5, Hs = -3	
0.0	-1.583322	-1.565389
0.1	-1.624076	-1.606043
0.2	-1.641463	-1.623380
0.3	-1.651107	-1.632993
S	M^2 = 2, $\alpha = 45^0$, ϕ = 0.01, γ = 0.1, b = 0.1, Hs = -3	
0.1	-1.441110	-1.430539
0.3	-1.531482	-1.517305
0.5	-1.624076	-1.606043
0.7	-1.718503	-1.696412
Hs	M^2 = 2, $\alpha = 45^0$, ϕ = 0.01, γ = 0.1, b =0.1, S = 0.5	
0	-1.590546	-1.572720
-1	-1.606746	-1.588801
-3	-1.624076	-1.606043
-5	-1.633904	-1.615832

From Table 3, one can notice that the skin friction coefficient at the wall decreases in magnitude with an increase in the angle of inclination and the velocity slip parameter for both Cu-water and Al_2O_3-water nanofluids. It is noticed that in the no-slip condition the highest wall shear stress occurs in magnitude.

Table 4 Variation in $-\frac{k_{nf}}{k_f}\theta'(0)$ for Cu - water and Al_2O_3-water nanofluids for different values of $M^2, \alpha, \phi, \gamma, b, S$ and H_s when λ = 1.5 and Pr = 6.2

M^2	$-\frac{k_{nf}}{k_f}\theta'(0)$	
	Cu- water nanofluid	Al_2O_3- water nanofluid
	$\alpha = 45^0$, ϕ = 0.01, γ =0.1, b =0.1, S = 0.5, Hs = -3	
0	4.178185	4.175867
1	4.160056	4.157336
2	4.146794	4.143889
4	4.127127	4.124037
α	M^2=2, ϕ = 0.01, γ= 0.1, b = 0.1, S = 0.5, Hs = -3	
0^0	4.143815	4.140925
30^0	4.145924	4.143024
45^0	4.146794	4.143889
60^0	4.147460	4.144552
ϕ	M^2=2, $\alpha = 45^0$, γ= 0.1, b = 0.1, S = 0.5, Hs = -3	
0.00	4.074657	4.074657
0.01	4.146794	4.143889
0.05	4.439210	4.424274
0.10	4.815724	4.784461
γ	M^2=2, $\alpha = 45^0$, ϕ = 0.01, b=0.1 S = 0.5, Hs = -3	
0.0	4.192285	4.188897
0.1	4.146794	4.143889
0.2	4.114164	4.111467
0.3	4.089356	4.086749
b	M^2=2, $\alpha = 45^0$, ϕ = 0.01, γ= 0.1, S = 0.5, Hs = -3	
0.0	6.946265	6.943669
0.1	4.146794	4.143889
0.2	2.956203	2.953720
0.3	2.296890	2.294782
S	M^2=2, $\alpha = 45^0$, ϕ = 0.01, γ= 0.1,b = 0.1, Hs = -3	
0.1	3.568487	3.566058
0.3	3.857252	3.854610
0.5	4.146794	4.143889
0.7	4.431778	4.428566
Hs	M^2=2, $\alpha = 45^0$, ϕ = 0.01, γ= 0.1, b=0.1, S = 0.5	
0	3.213419	3.213065
-1	3.617397	3.615674
-3	4.146794	4.143889
-5	4.509834	4.506302

However, the skin friction coefficient enhances in magnitude for both Cu-water and alumina-water nanofluids with increasing values of M^2, _, b, S and Hs. From the foregoing discussions, it is noticed that the skin friction coefficient in magnitude attains the higher values in case of Cu nanoparticles than that of Al_2O_3 nanoparticles.

It is observed from Table 4 that the reduced Nusselt number reduces with the increase in the magnetic interaction parameter, velocity slip and thermal jump parameters for both types of nanofluids. That is, as expected for the fluid flows at nanoscale, the rate of heat transfer at the wall decreases with an increase in the magnetic interaction parameter and the slip parameters. Moreover there is enhancement in the non-dimensional rate of heat transfer for increasing values of the angle of inclination, volume fraction, suction and heat absorption parameter for both types of nanofluids. It can also be seen from Table 4 that the reduced Nusselt number is positive for both types of nanofluids, and this is consistent with the fact that in the absence of viscous dissipation, heat flows from the surface of the fluid. Note that the entire values of $-\frac{k_{nf}}{k_f}\theta'(0)$ are always positive, i.e. the heat is transferred from the hot sheet to the cold fluid.

5. CONCLUSION

In this work, the problem of nonlinear hydromagnetic mixed convective nanofluid slip flow with heat transfer over an inclined stretching plate in the presence of internal heat absorption and suction is investigated. The numerical results are presented for the physical governing parameters including the magnetic parameter, angle of inclination, volume fraction, suction parameter, velocity slip parameter, thermal jump parameter and heat absorption parameter for both copper-water and alumina-water nanofluids. A systematic study on the effects of various parameters on the flow field, temperature, skin friction coefficient and the rate of heat transfer is carried out. From all the numerical computations, the main conclusions emerging from this study are as follows:

- The effect of magnetic field is to reduce the dimensionless velocity, skin friction coefficient and the non dimensional rate of heat transfer while its effect is to enhance the temperature. This is consistent with the fact that the momentum boundary layer thickness reduces with increasing M^2. However, the reverse effect is observed with the increase in the angle of inclination.
- Increase in volume fraction of copper-water nanofluid lead to retardation in the velocity and the opposite effect is noticed for alumina-water nanofluid. The inclusion of copper and aluminium nanoparticles into the base fluid has produced an enhancement in the temperature, skin friction coefficient in magnitude, reduced Nusselt number and as well as the thickness of the thermal boundary layer.
- The individual effect of both the suction parameter and heat absorption parameter is to reduce the velocity, temperature and the skin friction coefficient for both the copper-water and alumina-water nanofluids. But the non dimensional rate of heat transfer enhances with increasing values of both parameters.
- Increase in intensity of the velocity slip parameter γ leads to deceleration in the velocity and the the non dimensional rate of heat transfer while it accelerates the skin friction coefficient. The Momentum boundary

layer thickness is suppressed due to increasing values of the velocity slip parameter.

- The thermal jump parameter reduces the temperature, skin friction coefficient, the reduced Nusselt number and the thermal boundary layer thickness.
- The higher values of the skin friction coefficient and the reduced Nusselt number were obtained for copper nanoparticles compared to that of aluminium nanoparticles in the presence of heat absorption.

REFERENCES

Abu-Nada, E. and H. F. Oztop (2009). Effects of inclination angle1 on natural convection in enclosures filled with Cu-water nanofluid. *International Journal of Heat and Fluid Flow* 30, 669-678.

Akilu, S. and M. Narahari (2014). Effects of heat generation or absorption on free convection flow of a nanofluid past an isothermal inclined plate. *Advanced Materials and Research* 970, 267.

Alam, M. S., M. M. Rahman and M. A. Sattar (2006). MHD free convective heat and masstransfer flow past an inclined surface with heat generation. *Thammasat International Journal of Science and Technology* 11(4), 1–8.

Andersson, H. I. (2002). Slip flow past a stretching surface. *Acta Mechanica* 158, 121–125.

AnjaliDevi, S. P. and J. Andrews (2011). Laminar boundary layer flow of nanofluid over a flat plate. *International Journal of Applied Mathematics and Mechanics* 7(6), 52–71.

AnjaliDevi, S. P. and P. Suriyakumar (2013). Numerical investigation of mixed convective hydromagnetic nonlinear nanofluid flow past an inclined plate. *AIP Conference Proceedings* 1557, 281–285.

Aydin, O. and A. Kaya (2009). MHD mixed convective heat transfer about an inclined plate. *Heat and Mass Transfer* 46, 129–136.

Aziz, A. (2010). Hydrodynamic and thermal slip flow boundary layers over a flat plate with constant heat flux boundary condition. *Communications in Nonlinear Science and Numerical Simulation* 15, 573–580.

Bachok, N., A. Ishak and I. Pop (2010). Boundary layer flow of nanofluids over a moving surface in a flowing fluid. *International Journal of Thermal Sciences* 49,1663–1668.

Bachok, N., A. Ishak and I. Pop (2012).Boundary layer flow over a moving surface in a nanofluid with suction or injection. *Acta Mechanica Sinica* 28(1), 34–40.

Cao, K. and J. Baker (2009). Slip effects on mixed convective flow and heat transfer from a vertical plate. *International Journal of Heat and Mass Transfer* 52, 3829–3841.

Chamkha, A. J. and A. K. A. Rahim (2001). Similarity solutions for hydromagnetic simultaneous heat and mass transfer by natural convection from an inclined plate with internal heat generation or absorption. *Heat and Mass Transfer* 37,117–123.

Choi, S. U. S. (1995). Enhancing thermal conductivity of fluids with nanoparticles. *The proceedings of the ASME International Mechanical Engineering Congress and Exposition, San Francisco, USA, ASME, FED231/MD* 66, 99–105.

Das, K. (2012). Slip flow and convective heat transfer of nanofluids over a permeable stretching surface. *Computers and Fluids* 64, 34–42.

Das, S. K., S. U. S. Choi, W. Yu and T. Pradeep (2007). Nanofluids: Science and Technology. Inc., *Hoboken, New Jersey, USA: John Wiley and Sons*.

Fang, T., J. Zhang and S. Yao (2009). Slip MHD viscous flow over a stretching sheet an exact solution. *Communications in Nonlinear Science and Numerical Simulation* 14, 3731–3737.

Gebhart, B., Y. Jaluria, R. L. Mahajan and B. Sammakia (1988). Buoyancy induced flows and transports. *Chichester, UK.:Hemisphere Publishing Corporation*.

Haile, E. and B. Shankar (2015). A steady MHD boundary layer flow of water based nanofluids over a moving permeable flat plate. *International Journal of Mathematical Research* 4(1), 27–41.

Hamad, M. A. A. (2011). Analytical solution of natural convection flow of a nanofluid over a linearly stretching sheet in the presence of magnetic field. *International Communications in Heat and Mass Transfer* 38(4), 487–492.

Hassani, M., M. M. Tabar, H. Nemat, G. Domairry and F. Noori (2011). An analytical solution for boundary layer flow of a nanofluid past a stretching sheet. *International Journal of Thermal Sciences* 50(11), 2256–2263.

Hayat, T., M. Qasim and S. Mesloub (2011). MHD flow and heat transfer over permeable stretching sheet with slip conditions. *International Journal for Numerical Methods in Fluids* 66, 963–975.

Ishak, A., R. Nazar and I. Pop (2008). Hydromagnetic flow and heat transfer adjacent to a stretching vertical sheet. *Heat and Mass Transfer* 44, 921–927.

Kakac, S. and A. Pramuanjaroenkij (2009). Review of convective heat transfer enhancement with nanofluids. *International Journal of Heat and Mass Transfer* 52(13-14), 3187–3196.

Keshtkar, M. M. and B. Amiri (2013). MHD flow and heat transfer a nanofluid over a permeable stretching sheet. *International Journal of*

Engineering and Innovative Technology 3(3), 349–355.

Khan, W. A. and I. Pop (2010). Boundary layer flow of a nanofluid past a stretching sheet. *International Journal of Heat and Mass Transfer* 53, 2477–2483.

Martin, M. J. and I. D. Boyd (2006). Momentum and heat transfer in a laminar boundary layer with slip flow. *Journal of Thermophysics and Heat Transfer* 20(4), 710–719.

Mucoglu, A. and T. S. Chen (1979). Mixed convection on inclined surfaces. *Journal of Heat Transfer* 101, 422–426.

Noghrehabadi, A., M. Ghalambaz and A. Ghan barzadeh (2012). Heat transfer of magnetohydrodynamic viscous nanofluids over an isothermal stretching sheet. *Journal of Thermophysics and Heat Transfer* 26(4), 686.

Noor, N. F. M., S. Abbasbandy and I. Hashim (2012). Heat and mass transfer of thermophoretic MHD flow over an inclined radiate isothermal permeable surface in the presence of heat source/sink. *International Journal of Heat and Mass Transfer* 55, 2122-2128.

Oztop, H. F. and E. Abu-Nada (2008). Numerical study of natural convection in partially heated rectangular enclosures filled with nanofluids. *International Journal of Heat and Fluid Flow* 29, 1326–1336.

Rahman, M. M., M. A. Al-Lawatia, I. A. Eltayeb and N. Al-Salti (2012). Hydromagnetic slip flow of water based nanofluids past a wedge with convective surface in the presence of heat generation or absorption. *International Journal of Thermal Sciences* 57, 172–182.

Ramadan, H. M. and A. J. Chamkha (2003). Hydromagnetic free convection of a particulate suspension from a permeable inclined plate with heat absorption for non-uniform particle - phase density. *Heat and Mass Transfer* 39, 367–374.

Sharma, R., A. Ishak and I. Pop (2013). Partial slip flow and heat transfer over a stretching sheet in a nanofluid. *Mathematical Problems in Engineering* Article ID 724547, 1–7.

Srikanth, G. P. N., G. Srinivas and B. R. K. Reddy (2013). MHD convective heat transfer of a nanofluid flow past an inclined permeable plate with heat source and radiation. *International Journal of Physics and Mathematical Sciences* 3(1), 89–95.

Turkyilmazoglu, M. (2012). Exact analytical solutions for heat and mass transfer of MHD slip flow in nanofluids. *Chemical Engineering Science* 84, 182–187.

Wang, C. Y. (2002). Flow due to a stretching boundary with partial slip - an exact solution of the Navier-Stokes equations. *Chemical Engineering Science* 57, 3745–3747.

Wang, C. Y. (2009). Analysis of viscous flow due to a stretching sheet with surface slip and suction. *Nonlinear Analysis: Real World Applications* 10(1), 375–380.